

Characteristic of x-ray tomography performance using CdTe timepix detector

R. M. Zain, V. O'Shea, and D. Maneuski

Citation: [AIP Conference Proceedings](#) **1799**, 050013 (2017); doi: 10.1063/1.4972947

View online: <http://dx.doi.org/10.1063/1.4972947>

View Table of Contents: <http://aip.scitation.org/toc/apc/1799/1>

Published by the [American Institute of Physics](#)

Articles you may be interested in

[Image reconstruction of x-ray tomography by using image J platform](#)
AIP Conference Proceedings **1799**, 050010 (2017); 10.1063/1.4972944

[Slow neutron mapping technique for level interface measurement](#)
AIP Conference Proceedings **1799**, 050004 (2017); 10.1063/1.4972938

[Thorium fueled reactor](#)
AIP Conference Proceedings **1799**, 050012 (2017); 10.1063/1.4972946

[Dose measurement using Al₂O₃ dosimeter in comparison to LiF:Mg,Ti dosimeter and ionization chamber at low and high energy x-ray](#)
AIP Conference Proceedings **1799**, 040007 (2017); 10.1063/1.4972931

[Protection of people and environment from radiation risk through good regulatory practice](#)
AIP Conference Proceedings **1799**, 020004 (2017); 10.1063/1.4972902

[Characterization and attenuation study on tannin-added Rhizophora spp. particleboard at high energy photon and electron](#)
AIP Conference Proceedings **1799**, 040002 (2017); 10.1063/1.4972926

Characteristic of X-ray Tomography Performance using CdTe Timepix Detector

R.M. Zain^{1,a)}, V.O'Shea², D.Maneuski²

¹Malaysian Nuclear Agency, Bangi, 43000 Kajang, Selangor, Malaysia

²School of Physics & Astronomy, University of Glasgow, Scotland United Kingdom

^{a)}Corresponding author: rasif@nm.gov.my

Abstract. X-ray Computed Tomography (CT) is a non-destructive technique for visualizing interior features within solid objects, and for obtaining digital information on their 3-D geometries and properties. The selection of CdTe Timepix detector has a sufficient performance of imaging detector is based on quality of detector performance and energy resolution. The study of Modulation Transfer Function (MTF) shows a 70% contrast at 4 lp/mm was achieved for the 55 μm pixel pitch detector with the 60 kVp X-ray tube and 5 keV noise level. No significant degradation in performance was observed for X-ray tube energies of 20 – 60 keV. The paper discusses the application of the CdTe Timepix detector to produce a good quality image of X-ray tomography imaging.

Keywords: X-ray tomography, radiation detector, timepix, tomogram

INTRODUCTION

A semiconductor CdTe material has been considered as a smart and an appropriate detector for room temperature x-ray and gamma-ray detectors. Its high band gap, relatively high density and atomic weight, high resistivity entailing a low leakage current, and most importantly, its electron drift length has brought it to the attention of researchers and entrepreneurs [1]. CdTe detectors are known for their high radiation-detection efficiency, position sensitivity, high stopping power, good energy-resolution, low power- consumption, low electronic-noise and portability at room temperature. All these required characteristics for a reliable radiation detector make CdTe a good material for x- ray and gamma-ray-detectors in a variety of fields, such as industrial quality control, non destructive testing imaging, medical imaging, space and astronomy.

In this study the CdTe material was bump-bonded to the 65k pixel Timepix readout ASIC [1]. The chip has several readout modes including single photon counting and energy discrimination mode. The CdTe Timepix detector shown the high quality image of X-ray tomography. In order to prove its performance, the results reported here assess both detector performance and spectroscopic performance capabilities for 55 μm .

THE STRUCTURE OF THE TIMEPIX

The Timepix chip has a pixelated array of 256X256 pixels each containing an analog and a digital part. The chip has a power consumption of 440 mW and 450 mW for the analogue and digital sections respectively, for a reference clock frequency of 80 MHz [2]. To facilitate tiling the chip, the pixel array is placed on one side of the chip, leaving three sides which have less than 50 μm inactive spaces between the pixels and the physical edge of the chip. The digital readout section on the periphery contains wire-bonding pads and the control logic for input and output. It also has contains the circuitry to generate all of the bias/control voltages and currents needed for the operation of the chip. There are 13 global digital to analog converters (DAC), of which eight are 8-bit current DACs, and four are 8-bit voltage DACs. There is a linear voltage DAC, which sets the threshold (THL) using 14 bits. This DAC is split in an overall threshold setting of 10-bit, and 4-bit for adjustments of the threshold for each individual pixel. In this way, variations between pixels can be equalised [3].

Each individual pixel is 55X55 μm^2 in size and contains an analogue and a digital section. Figure 1 shows the block diagram of a Timepix pixel cell. The analog part contains a pre-amplifier, discriminator and a 4-bit threshold adjustment. The digital side of the pixel consists of the counting logic, synchronisation logic for the reference clock, overflow control logic, a buffer and a pixel configuration register for setting the acquisition

mode and the threshold equalisation. The synchronisation logic has three operation modes (counting, ToA and ToT) which can be set by the configuration bits P0 and P1 [4].

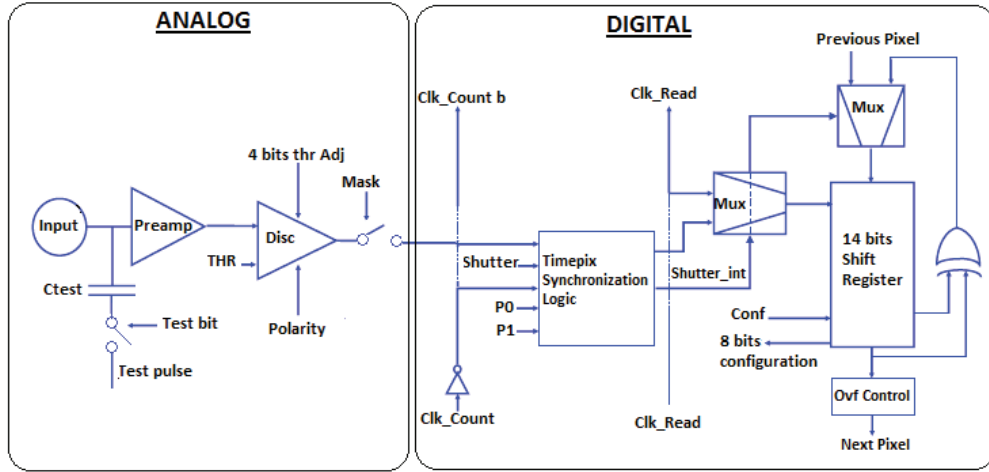


FIGURE 1. Timepix pixel schematic [2][5].

IMAGING PERFORMANCE (MTF)

The MTF characterises the spatial frequency response of an imaging system and basically describes how well the object contrast is transmitted through the imaging chain for a given spatial frequency. It is defined as the ratio between the modulation of a sinusoidal test pattern M_{in} at a spatial frequency f and the modulation of the obtained image, M_{out} :

$$MTF(f) = \frac{M_{out}(f)}{M_{in}(f)} \quad (1)$$

It yields a value between zero and 1 for all frequencies and can be described by analytical functions or a convolution of functions in simple cases [6]. Assuming for example square pixels with lateral dimension l and a uniform sensitivity over the whole pixel area, the theoretical limit for the MTF is given by:

$$MTF_{sq} = \frac{\sin(\pi fl)}{\pi fl} =: sinc(\pi fl) \quad (2)$$

where f denotes the spatial frequency. There are two methods for measuring the MTF of a given system: the edge method and the slit method [7].

The edge method is a relatively fast and easy method to derive the MTF of a digital imaging system from a single, even a rather small, image. This is especially convenient when working with small detectors and at an early development stage [2]. For this method a precision edge made from e.g. tungsten is placed approximately 1.5° tilted to the pixel rows over the detector and an image is acquired. By projecting the image data along the direction of the edge, a one-dimensional oversampled data set is obtained from which the edge spread function is determined and numerically differentiated, leading to the line spread function (LSF) perpendicular to the edge. Calculating the modulus of the Fourier transform of the LSF results in the desired MTF, which is also perpendicular to the edge.

The slit method uses a fine slit instead of the edge employed when using the edge method [8]. The advantage of the slit method when compared to the edge method is that the projection of the image data along the slit axis leads directly to the LSF without the need to calculate the derivative of the edge spread functions. But it has also disadvantages: the fabrication of a fine, accurate slit is more difficult than that of a simple edge and the lowest frequency components are not readily available in the image because only a very narrow strip of the detector is illuminated. To evaluate the measurement the low frequency components of the LSF must be extrapolated [9]. Last but not least the positioning of the slit can be rather more difficult because only a nearly perfect alignment produces a satisfactory slit image; the side walls of the slit must be oriented exactly perpendicular to the detector plane for the slit to be seen at all. On the other hand it is not easy to achieve a very good alignment when using a single edge since the edge image does not show misalignments so clearly.

For the Modulation Transfer Function (MTF) measurements the bremsstrahlung spectrum from a dental X-ray tube operated at 60 kVp was used. No flat field correction of the acquired images was performed. This approach was chosen in order to establish the basic performance of the system without any corrections.

RESULTS AND DISCUSSION

A comparison between MTFs at various bias voltages for the 55 μm pitch detector is presented in Figure 2. Meanwhile, Figure 3 (a) and (b) shows the variation of image quality, corresponding to two bias voltages of -100 and -500 V respectively. From the result, the best MTF is observed for bias voltages of 400–500 V. Gradual degradation of performance is seen for smaller detector biases. It should be noted that due to non-uniformities and defects in the detector material a variation of 10 – 20% in the MTF taken from various “good” regions on the detector was observed.

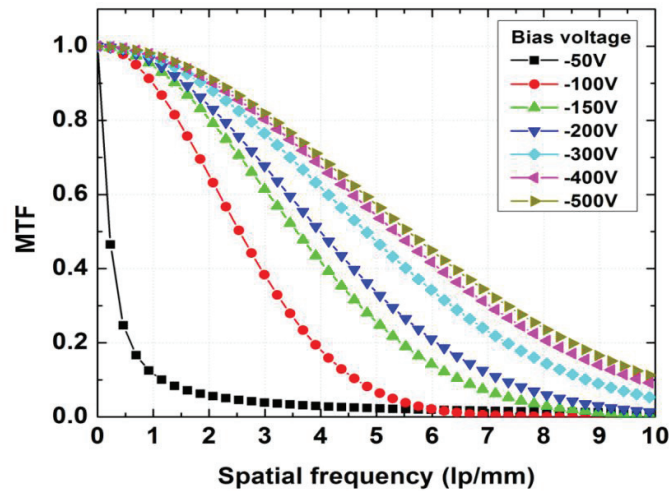


FIGURE 2. MTF dependence of bias voltage recorded by the 55 μm pixel pitch sensor. X-ray tube energy was set up to 60 kVp.

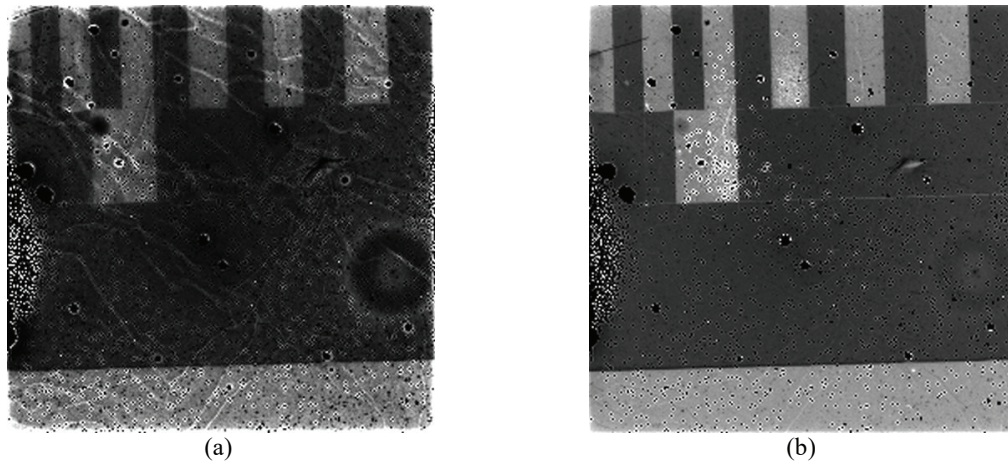


FIGURE 3. Images to the right demonstrate the quality of the image recorded: (a) at -100V and (b) -500V.

The MTF performance was assessed at various X-ray tube cathode voltages. A degradation of ~10% was observed for X-ray tube energies ranging from 20 and up to 60 kVp, which is mainly associated with the $PbNr$ being more transparent at higher energies, leading to a degradation of the edge quality. This pattern can be seen in Figure 4.

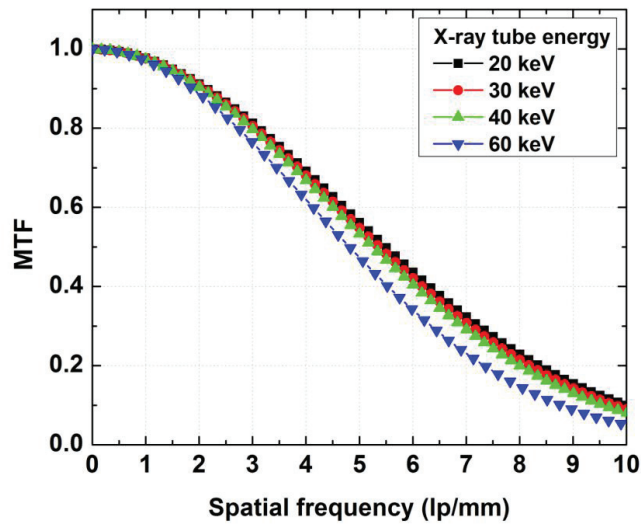


FIGURE 4. 55 μm pixel detector MTF dependence on X-ray tube voltage. The detector was biased at -300 V , threshold was set to $\sim 5\text{ keV}$.

The tomogram voltage regulator by using of CdTe Timepix detector shown in Figure 5. The results show a good quality of a three- leg connector tomogram of voltage regulator inside the housing being visualized. This technique is beneficial for quality control in applications such as industrial production [1].

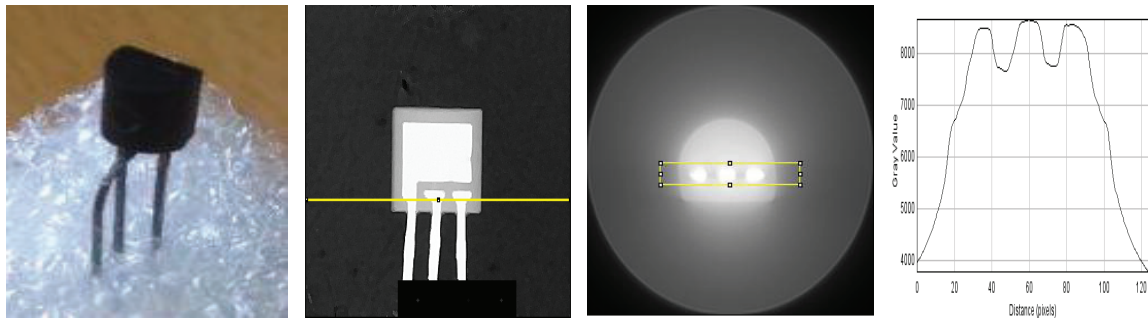


FIGURE 5. Tomogram of voltage regulator.

CONCLUSION

In this study the pixellated CdTe Timepix detector has shown that it is capable of performing X-ray tomography producing images of high quality. The CdTe detector with $55\ \mu\text{m}$ pitch demonstrates reasonable imaging performance. A 70% contrast at $4\ \text{lp/mm}$ was achieved for the $55\ \mu\text{m}$ pixel pitch detector with the 60 kVp X-ray tube and 5 keV noise level. No significant degradation in performance was observed for X-ray tube energies of 20 – 60 keV.

REFERENCES

1. Dzmityr Maneuski, V Astromskas, E Fröjd, C Fröjd, Eva Gimenez-Navarro, Julien Marchal, V O'Shea, G Stewart, Nicola Tartoni, Heribert Wilhelm, K Wraight, R M Zain, "Imaging and spectroscopic performance studies of pixellated CdTe Timepix detector," in *Journal of Instrumentation* 7, doi 10.1088/1748-0221/7/01/C01038
2. Xavier llopart, Timepix manual V1.0, file :Timepix manualV1.0.pdf

3. X. Llopart, M. Campbell, R. Dinapoli, D. San Segundo and E. Pemigotti, "Medipix2: a 64-k pixel readout chip with 55 μm square elements working in single photon counting mode," in *IEEE Transactions on Nuclear Science*, vol.49, no. 5, pp.2278-2283 (2002).
4. X. Llopart, R. Ballabriga, M. Campbell, L. Tlustot and W. Wong, "Timepix, a 65k programmable pixel readout chip for arrival time, energy and/or photon counting measurements," in *Nuclear Instruments and Methods in Physics Research A*, vol. 581, pp.485-494 (2007).
5. Z. Vykydal, J. Jak_ubek and S. Pospsil, "USB Interface for Medipix2 Pixel Device Enabling Energy and Position Detection of Heavy Charged Particles," in *Nuclear Instruments and Methods A*, vol. 536. pp. 112-115 (2006).
6. Joseph M. Geary, "Chapter 34 – MTF: Image Quality V," in *Introduction to Lens Design: With Practical Zemax Examples*, 389-96. Richmond, VA: Willmann-Bell (2002).
7. Hecht, Eugene. "11.3.5 Transfer Functions," in *Optics*, 550-56. 4th ed. San Francisco, CA: Addison-Wesley (2001).
8. Warren J. Smith, "Chapter 15.8 The Modulation Transfer Function," in *Modern Optical Engineering*, 385-90. 4th ed. New York, NY: McGraw-Hill Education (2008).